

УДК 524.7—82

TWO-COLOUR PHOTOMETRY OF CLUSTERS OF GALAXIES. I  
A1185

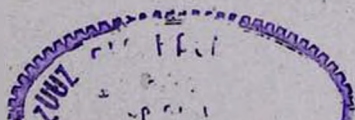
A. T. KALLOGHLIAN, A. G. EGIKIAN, D. NANNI, D. TREVESE, A. VIGNATO

Received 15 November 1982

Accepted 27 January 1983

The results of two-colour photometry in  $B$  and  $V$  of galaxies in A1185 are presented. The plates of the 2.6 m telescope of the Byurakan Observatory have been used. The measurements were carried out with the PDS microdensitometer of the Naples Observatory. The rectangular coordinates, total magnitudes and colours, ellipticities and position angles of large axes of galaxies have been determined. The luminosity functions in  $B$  and  $V$  are constructed. There is a change of slope in cumulative luminosity functions in both  $B$  and  $V$  at  $M_B^* = -19^m0$  and  $M_V^* = -20^m0$  respectively. No convincing evidence has been found for preferential alignments of galaxy axes. The brighter and redder the galaxies the stronger is the concentration to the cluster centre.

1. *Introduction.* In the last decade quite a large number of clusters of galaxies have been studied photometrically. Extensive investigations have been carried out by Oemler [1], Dressler [2], Godwin and Peach [3], Carter [4], Carter and Godwin [5], Hoffman and Crane [6], Kron [7] and others in order to reveal global photometric parameters of clusters. Unfortunately the results of several photometry have been published in an incomplete form which makes them difficult to compare with other data. Usually the photometry refers to one or another colour band which in turn differs from one article to another. This is another trouble for comparison. Nevertheless by means of photometry various general properties such as structure, shape of luminosity function, segregation effects and others have been obtained which are important to understand the problems related to the formation and evolution of clusters of galaxies. A photometry at least in two colour bands should be more informative. Taking this into account a photometric study in  $B$  and  $V$  has been undertaken for several clusters of galaxies from Abell's list [8]. In this paper we give the results on cluster A1185.



According to Abell [8] the cluster A1185 belongs to the richness class 1 and distance group 2. It means that in radius 50 arcmin (hereafter  $H = 75 \text{ km s}^{-1} \text{ Mpc}^{-1}$ ) the cluster has about 50–79 members in a magnitude range ( $m_3, m_3 + 2$ ), where  $m_3$  is the magnitude of the third brightest member. The field measured in this article has angular sizes equal to  $35 \times 35 \text{ arcmin}^2$ . The cluster belongs to Bautz-Morgan type II [9] with a redshift 0.0349 [10]. The brightest member of the cluster is NGC 3550 by means of which the cluster redshift is measured. The cluster is a weak radio source [11, 12]. It was not detected in X-ray observations [13]. According to [14] A1185 is a member of a double cluster, the second member being A1213. A1185 has not been investigated photometrically.

2. *Observations.* Measurements of galaxies were made on plates taken at the prime focus of the 2.6 m telescope of the Byurakan Observatory. The plate scale is 21.4 per mm, while the corrected field has a diameter of about 45 arcmin. Only the central field of 35 arcmin diameter has been measured. The photometry is based on a 30 min Kodak 103a-0+GG385 plate for *B* band and a 40 min Kodak 103a-D+GG11 plate for *V* band.

Photometric calibration of the plates has been performed by means of the Byurakan Observatory 12-tube spot sensitometer of known relative intensities. The calibrating exposure was made after the sky exposure on a masked-off part of the plate. Usually 6 or 7 spots were normally exposed for measurements. To establish the zero points for photometry, the sky background surface brightnesses measured photoelectrically and photographically (by means of standard stars in star cluster IC 4665) have been used.

The combination of used filters and plates together with atmosphere defines a colour system very near to the standard *BV* system. No correction for this slight difference has been made.

3. *Reduction procedures.* a) *Plate scanning.* The plates were scanned with the PDS microdensitometer of the Naples Observatory.

The aperture used for the scanning was a square one of  $25 \times 25$  microns; also the step in *x* and *y* was 25 microns. The step and aperture correspond approximately, at the scale of the telescope, to about  $0.5''$ . The region scanned is a square of  $10 \times 10 \text{ cm}$  which correspond to  $35' \times 35'$ . Therefore the scanning gives rise to a matrix of  $4000 \times 4000$  numbers. We adopt the transparency mode on the microdensitometer because, in this way, we have a good sampling near the background value which, in turn, gives rise to an accurate evaluation of luminosity of galaxies near the plate limit.

b) *Segmentation process.* A finder program retrieves individual objects discriminating them from background and determining their positions and sizes: the objects are defined as connected areas of a certain number of pixels overcoming a suitable threshold level. The details of the algorithm were described by Pittella and Vignato [15]. Some improvements were introduced in the procedure, as described there, in the attempt of eliminating the inconveniences connected with: a) the presence of a certain number of double objects, this presence is due to the choice of a low value of the threshold opacitance that we used not to loose the faintest objects, b) a number of objects introduced (or missed) in the final catalogue due to discontinuity in the background level from one region to another one, the background level being, in fact, computed as the modal value of the histograms evaluated in adjacent cells of typical dimension  $100 \times 100$  pixels.

After some attempts we found this procedure suitable: 1) the original image ( $4000 \times 4000$ ) was squeezed to  $1000 \times 1000$  by averaging; this reduces the noise still preserving enough spatial resolution; 2) a second image  $1000 \times 1000$  was produced by smoothing the previous one with a  $3 \times 3$  mask. This second image is used only for the finding of algorithm like a local background. Then an image is produced by dividing the transparency of each pixel of the second image by the transparency of the corresponding pixel of the first one. To this last image the old finding procedure is applied. This procedure avoids the inconveniences of the previous method and, in particular, very faint objects may be detected also if embedded in the envelope of a luminous one.

c) *Calibration.* The calibration performed on the plate was made using the spots present on it. We found convenient to use the following variable:

$$\mathcal{Q} = (D - D_f) / (D_s - D) \quad (1)$$

with this meaning for the symbols:

$$D = -\log T$$

$$D_f = \text{fog density}$$

$$D_s = \text{saturation density.}$$

We note that the variable  $\mathcal{Q}$  for values of density much less than the saturation density is the same as the Becker density. Moreover the relation

$$I = a\mathcal{Q}^n \quad (2)$$

that we used to calibrate the plate gives rise in the density-log I diagram to the classical S-shape relation.

d) *Photometry*. The magnitudes of the objects were computed inside circular diaphragms of different apertures; the centers of the objects were recomputed on the original image starting from the  $x$  and  $y$  values given by the finding algorithm. For the objects with a nearby companion we take into account the presence of this object by rejecting, for each annulus, having a radius greater than a certain value, the opacitance values outside the dispersion from the mean and substituting in them the mean opacitance of the remaining pixels.

The intensity for each pixel has the form

$$i = (I - I_r) / I_b \quad (3)$$

where  $I_r$  is the intensity due to light not belonging to the object; it corresponds to the sum of the background intensity  $I_b$  and the diffuse light of the underlying objects.

After the computation of the magnitude inside circular diaphragms, we analyze the behaviour of magnitude versus radius and we consider as the "total" magnitude that one for which the stability of the magnitude values was achieved inside the error induced by the photographic noise.

By our measurements within a diameter of 42.8 arcsec the  $V$  magnitude of NGC 3550 (No. 1 in Table 1) is equal to  $13^m64$ . This can be compared with the value  $V = 13.58$  obtained by Peterson within an aperture 41.8 arcsec [16].

We also computed the ellipticity and position angle for the objects using the scheme outlined by Carter and Metcalfe [17].

e) *Star-galaxy separation*. Many techniques are used to discriminate between stars and galaxies; these methods seem to fall into two categories;

1) the ones based on assumed model of intensity profile of a certain type of objects (in general stars). These methods were used by Lorre et al [18], and quite recently by Valdes [19].

2) other methods are based on morphological parameters of the discrimination criteria being the manifestation of the fact that the star is a point spread function (PSF) while galaxies are extended sources convolved with the PSF. Peterson et al [20] based their classifier on the areal profiles of the images. Kron [7] used the parameter  $r$  which weights the central light strongly

Table 1

MAGNITUDES AND COLOURS OF GALAXIES IN A1185

No.	$X_V$	$Y_V$	$V$	$B-V$	No.	$X_V$	$Y_V$	$V$	$B-V$
1	-190 <sup>m</sup>	+375 <sup>m</sup>	13. <sup>m</sup> 64	1. <sup>m</sup> 14	38	559 <sup>m</sup>	- 379 <sup>m</sup>	16. <sup>m</sup> 65	0. <sup>m</sup> 93
2	31	-457	14.20	1.10	39	78	- 586	15.66	0.99
3	-167	67	14.35	0.87:	40	575	519	16.67	0.72
4	274	104	14.36	1.10	41	- 480	465	16.67	0.91
5	-135	99	14.52	1.06	42	- 280	462	16.74	0.77
6	- 70	- 24	14.57	1.10	43	363	- 534	16.86	0.89
7	968	-700	14.71	0.56	44	519	- 98	16.86	0.65
8	-205	246	14.94	1.10	45	-1005	58	16.89	0.76
9	272	161	14.96	0.91	46	- 855	249	16.91	0.85
10	-971	955	14.96	1.11	47	- 216	140	16.91	0.99
11	425	228	14.98	1.13	48	793	- 317	16.94	0.60
12	355	45	15.20	1.03	49	587	125	16.97	0.78
13	- 12	132	15.24	1.22	50	322	1052	17.0	-
14	-433	-143	15.26	1.17	51	- 5	- 262	17.05	0.93
15	-156	-778	15.54	0.97	52	978	141	17.08	1.32
16	-346	109	15.59	1.09	53	77	160	17.09	1.10
17	-355	82	15.64	1.07	54	904	- 23	17.17	0.57
18	19	-737	15.65	0.64	55	949	515	17.21	0.81
19	77	37	15.65	1.07	56	- 633	1027	17.23	0.78
20	91	287	15.67	1.06	57	- 21	472	17.24	-
21	577	280	15.74	0.77	58	715	921	17.27	1.45
22	13	-388	15.74	1.08	59	472	- 291	17.34	1.02
23	-377	159	15.81	0.86	60	863	- 689	17.38	0.67
24	-601	-195	15.93	0.55	61	494	- 195	17.44	0.59
25	- 87	96	15.96	1.00	62	- 698	302	17.48	0.73
26	-307	124	16.16	1.02	63	- 240	132	17.49	0.85
27	562	316	16.18	1.15	64	- 302	- 572	17.50	0.89
28	-271	-646	16.20	0.67	65	- 144	350	17.51	0.78
29	-483	-348	16.29	0.77	66	518	1008	17.53	1.33
30	376	11	16.33	0.70	67	407	194	17.55	-
31	-132	866	16.33	0.89:	68	- 188	731	17.59	1.45
32	-174	151	16.35	1.02	69	915	- 798	17.59	1.01
33	634	559	16.44	1.07	70	183	68	17.59	0.58
34	-140	-224	16.45	1.15	71	- 366	209	17.63	1.03
35	427	-490	16.47	0.81	72	277	72	17.71	0.56
36	762	-270	16.52	0.75	73	190	- 695	17.74	0.66
37	-557	-715	16.59	0.98	74	- 626	916	17.74	0.87

Table 1 (continued)

No.	$X_V$	$Y_V$	$V$	$B-V$	No.	$X_V$	$Y_V$	$V$	$B-V$
75	-174 <sup>m</sup>	331 <sup>r</sup>	17 <sup>m</sup> .77	0 <sup>m</sup> .90	113	162	-552	18 <sup>m</sup> .44	0 <sup>m</sup> .81
76	-314	-1011	17.8	-	114	-990	-354	18.44	1.20
77	-389	206	17.82	0.76	115	398	-223	18.44	-
78	656	768	17.83	1.37	116	-158	-852	18.45	-
79	-877	-613	17.84	0.48:	117	674	568	18.45	1.35
80	671	974	17.88	1.59	118	-458	184	18.46	-
81	-204	118	17.88	0.85	119	5	-189	18.47	1.48
82	-461	204	17.89	1.48	120	73	259	18.47	0.84
83	-46	523	17.90	0.35	121	195	-599	18.48	-
84	134	869	17.91	0.58	122	131	-524	18.49	0.71
85	-775	226	17.91	0.82	123	378	-150	18.52	0.95
86	-325	-703	17.91	0.83	124	508	874	18.53	0.14
87	278	-711	17.93	0.76	125	-349	-984	18.53	1.23
88	-276	603	17.96	0.40	126	-548	-14	18.53	-
89	-101	-166	18.02	1.77	127	-494	-914	18.56	0.98
90	327	295	18.03	-	128	74	-627	18.57	0.54
91	552	633	18.05	0.70	129	-610	-840	18.58	0.63
92	-496	376	18.06	1.01	130	251	276	18.58	1.43
93	-317	807	18.06	1.57	131	-530	20	18.60	-
94	126	-223	18.08	1.17	132	-486	791	18.64	1.43
95	172	287	18.09	1.32	133	228	696	18.68	-0.08
96	-945	772	18.10	1.16	134	-686	-14	18.69	0.49
97	263	171	18.10	-	135	-579	823	18.71	0.88
98	235	861	18.10	-	136	937	564	18.71	-
99	222	-279	18.13	1.58	137	-482	1025	18.71	0.75
100	888	-97	18.13	-	138	-728	-887	18.72	-
101	-1040	-405	18.23	1.47	139	262	135	18.72	-
102	-123	-547	18.23	0.74	140	229	683	18.74	-
103	874	-448	18.27	0.59	141	22	283	18.75	0.30
104	398	388	18.27	0.40	142	-484	150	18.76	-
105	-670	-222	18.31	1.29	143	-482	151	18.79	-
106	-891	622	18.35	0.67	144	796	-111	18.79	-
107	472	690	18.37	-0.08	145	-84	331	18.79	-
108	-959	-410	18.39	-	146	239	616	18.79	0.87
109	-37	422	18.39	-	147	75	506	18.91	0.41
110	-868	201	18.40	-	148	256	166	18.82	0.12
111	-101	97	18.41	0.56	149	242	-502	18.82	-
112	-240	-564	18.44	0.60	150	-608	-545	18.83	-

Table 1 (continued)

No.	$X_V$	$Y_V$	$V$	$B-V$	No.	$X_V$	$Y_V$	$V$	$B-V$
151	330 <sup>m</sup>	-490 <sup>m</sup>	18. <sup>m</sup> 84	—	189.	790	973 <sup>m</sup>	19. <sup>m</sup> 34	0. <sup>m</sup> 67
152	-637	-853	18.84	0. <sup>m</sup> 40	190	921	133	19.38	—
153	-328	779	18.85	—	191	378	-366	19.38	—
154	-374	974	18.86	—	192	672	299	19.39	—
155	-635	585	18.86	0.58	193	-645	425	19.40	—
156	-373	311	18.89	—	194	-969	399	19.40	—
157	159	-679	18.92	—	195	612	17	19.40	0.37
158	3	441	18.94	—	196	-681	-389	19.40	—
159	-412	172	18.94	—	197	-120	-58	19.43	—
160	-779	875	18.95	—	198	187	384	19.44	—
161	-198	-442	18.96	0.73	199	-636	327	19.45	1.25
162	912	-349	18.97	—	200	-781	-760	19.45	—
163	133	-996	18.97	—	201	670	-813	19.46	—
164	394	-608	18.97	—	202	-693	630	19.47	0.52
165	-169	-189.	18.98	—	203	921	164	19.47	—
166	124	607	19.01	—	204	-912	253	19.48	—
167	-344	70	19.04	—	205	551	-143	19.50	—
168	508	-234	19.05	0.37	206	-20	-500	19.50	—
169	-93	626	19.06	—	207	-809	-530	19.51	—
170	213	867	19.07	—	208	-276	-942	19.55	—
171	200	274	19.11	—	209	957	-417	19.55	—
172	-492	77	19.13	—	210	-738	191	19.58	—
173	576	-939	19.14	—	211	-985	-308	19.60	—
174	-546	225	19.16	—	212	-403	-124	19.72	—
175	-66	-744	19.18	—	213	-475	36	19.72	—
176	-804	662	19.20	—	214	569	615	19.73	—
177	4	281	19.21	0.63	215	610	946	19.77	—
178	708	-537	19.25	0.61	216	6	-267	19.80	—
179	-219	-170	19.27	—	217	-121	716	19.81	—
180	669	-933	19.29	—	218	56	-515	19.85	0.57
181	-322	20	19.31	—	219	-879	999	19.87	0.09
182	794	608	19.31	—	220	-88	-316	19.91	0.68
183	-675	593	19.31	—	221	-863	307	19.93	—
184	443	-610	19.32	0.54	222	-696	113	19.93	—
185	167	-83	19.33	—	223	765	-106	19.96	—
186	-262	-159	19.33	—	224	-295	-967	19.97	—
187	563	29	19.33	—	225	477	338	20.32	—
188	53	-605	19.34	—					

$$r = \left\{ \int_0^{2\pi} d\theta \int_1^{\bar{r}} l^{-2} f(l, \theta) l dl / \int_0^{2\pi} d\theta \int_1^{\bar{r}} f(l, \theta) l dl \right\}^{-1/2}, \quad (4)$$

where  $f$  is the light distribution and  $l$  is the distance from the centroid of the object.

In the past Nanni et al. [21] used also a model-free parameter, mainly the second opacitance moment. Here to discriminate stars from galaxies we use the difference between the magnitudes of an object at different radii; the value used for the radii were chosen in an empirical way and correspond, approximately, the first to the radius of the seeing disk and the second to 3 times this value. The histogram of

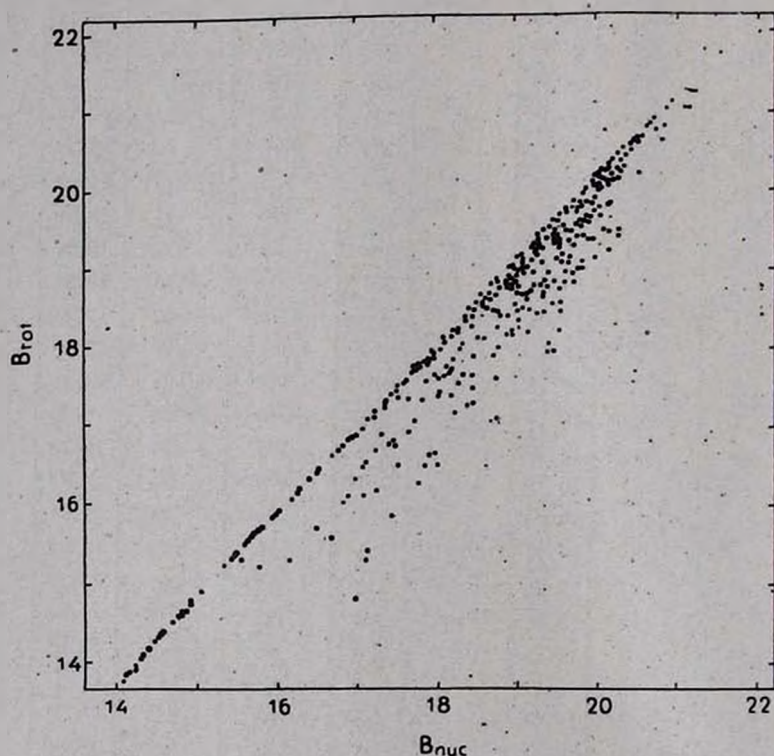


Fig. 1. Star-galaxy separation.

Fig. 1 shows that in this way, a reliable separation between stars and galaxies is achieved up to  $20^m7$  for the blue plates while the limiting magnitude for these plates is approximately  $21^m7$ .

4. *Results.* 143 galaxies have been identified in both  $B$  and  $V$  and 225 galaxies only in  $V$  within a circular area of diameter 35 arcmin centered on Abell's position. A finding chart is presented in Fig. 2.

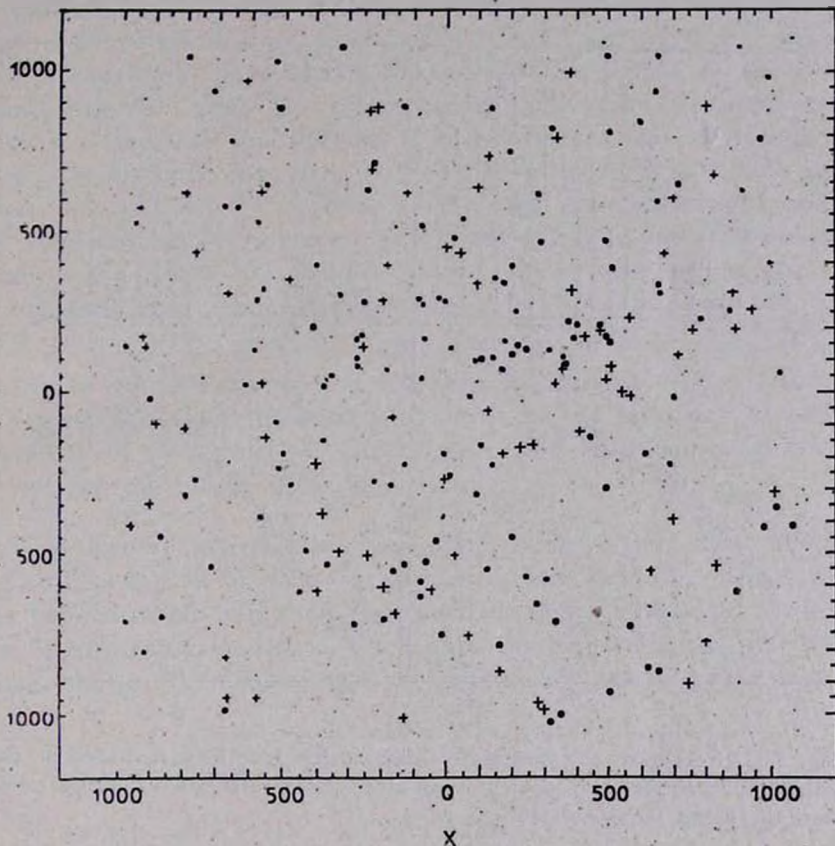


Fig. 2. Identification chart of galaxies in A 1185; filled circles—galaxies identified in  $B$  and  $V$ , crosses—galaxies identified only in  $V$ .

Current numbers,  $X$  and  $Y$  rectangular coordinates with respect to Abell's center, total  $V$ -magnitudes, the corresponding  $B-V$  colours of galaxies are given in Table 1. The completeness limits in  $B$  and  $V$  are  $19^m.0$  and  $18^m.6$  respectively.

For field corrections Karachentsev's and Koplov's [22] and Kron's data [7] have been used. The field correction predicts 24 and 49 galaxies which are brighter than the completeness limits in  $B$  and  $V$  respectively and seem to be non-members within the measured area.

a) *The luminosity function.* Fig. 3 shows the differential and cumulative luminosity functions of A1185 in  $B$  and  $V$ . The completeness

limits are marked by vertical dotted lines. The effect of corrections for non-members are also shown. As it is seen, the application of field correction does not change the general form of luminosity functions considerably in both colours though its effect becomes dominant for

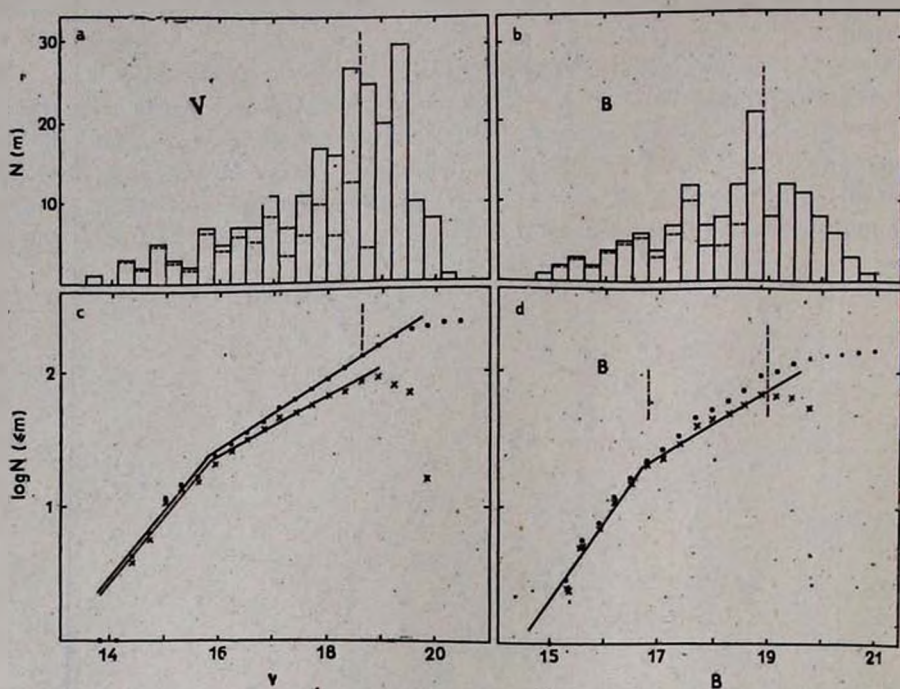


Fig. 3. Differential and cumulative luminosity functions in  $B$  and  $V$ . Solid lines—without field corrections, dotted lines—after field corrections. Vertical dotted lines show the limits for completeness.

faint magnitudes. The luminosity function in  $B$  and  $V$  is comparatively flat at the bright end. Compared to the luminosity function of Coma cluster, this flatness is quite significant. The slope in cumulative luminosity function of A1185 changes at the bright end of the curves due to a local minimum in differential function. This means that the functions in Fig. 3 cannot be represented by a monotonically rising analytic approximation as that proposed by Schechter [23]. The points of changing the slopes in cumulative luminosity functions in  $B$  and  $V$  have apparent magnitudes  $16^m.8$  and  $15^m.8$  respectively. Using the known redshift of the cluster the corresponding absolute magnitudes are  $-18^m.9$  and  $-19^m.9$ . This may be compared with values of  $M_V^* = -20.3$  given by Abell [24], and  $M_V^* = -20.1$  given by Godwin and Peach [3]

for Coma cluster referring to the same value of Hubble constant. If a correction for galactic absorption is applied we obtain  $M_V = -20.0$  for A1185. Taking into account the differences in magnitude reduction methods and apparently in colour systems the agreement between the data is fairly good.

The straight lines in Fig. 3c and 3d are fitted to the corrected points brighter than the completeness limit and have slopes 0.57 and 0.25 in  $B$  and 0.49 and 0.21 in  $V$  at the bright and faint ends respectively. In both colours the first points with  $\log N = 0$  have not been taken into account. For Coma cluster the corresponding slopes in  $V$  are 0.85 and 0.18, obtained by Abell [24] and 0.64 and 0.25 obtained by Godwin and Peach [3]. Abell's value for the faint end of the cumulative logarithmic luminosity function refers to the magnitude interval  $14^m5 < m_V \leq 17^m5$ . There is a second change of slope at  $m_V = 17^m5$  the reality of which however has not been established. As it is seen there is a good agreement between the slopes at the faint end of luminosity functions of both clusters. The bright end of the luminosity function is flatter for the cluster A1185.

b) *Radial distribution and segregation effects.* To discuss the radial distribution of galaxies in the cluster field the measured region has been divided into several concentric rings. Results of these counts are demonstrated in Fig. 4. On x-axis the ring radius is plotted, while y-axis shows the relative number of galaxies per square arc degree.

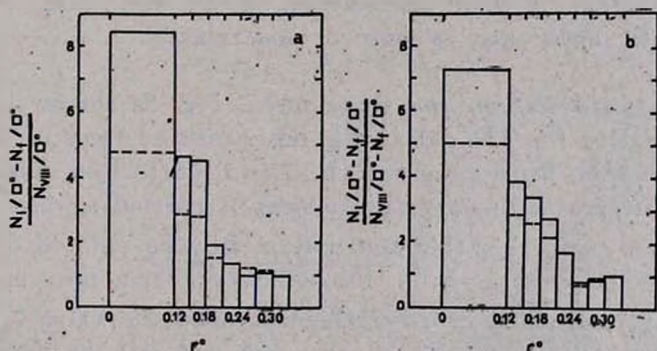


Fig. 4. Radial distribution of galaxies; dotted lines-without field correction, solid lines-after field correction; a) the total number of galaxies is 131 until the completeness limit in  $V$ ; b) the total number of galaxies identified both in  $B$  and  $V$  is 94.

The galaxy density in the outer ring is taken as unity. The total number of galaxies used in Fig. 4a is 131 until the completeness limit in  $V$ .

The observed ratio of galaxy densities in central and outer rings is about 5 while after field correction it becomes more than 8. The field correction has been applied according to Karachentsev's and Kopilov's data [22] for each magnitude interval in every ring.

Radial distribution of 94 galaxies identified in  $V$  as well as in  $B$  until the completeness limit of the latter is shown in Fig. 4b. No significant difference between two distributions exists.

To investigate the luminosity segregation effect in the cluster, the ratio of numbers of galaxies brighter and fainter than a certain magnitude has been determined. As border magnitudes  $16^m$ ,  $16^m.5$  and  $17^m.0$  have been taken subsequently. The results are shown in Table 2.

Table 2

LUMINOSITY SEGREGATION EFFECT IN THE  
CLUSTER A1185

Ring	$\frac{n_{V<16}}{n_{16<V<18.6}}$	$\frac{n_{V<16.5}}{n_{16.5<V<18.6}}$	$\frac{n_{V<17}}{n_{17<V<18.6}}$
	0—0.12	0.64	0.95
0.12—0.24	0.15	0.29	0.70
0.24—0.33	0.06	0.09	0.23

No field correction has been applied to these data. Total number of galaxies used in Table 2 is 131 until the completeness limit in  $V$ . As it is seen significant luminosity segregation exists in all three cases, although the effect is less predominant in the third case. This means that the cluster apparently is more or less relaxed.

c) *Colour distribution and segregation.* Fig. 5a shows the integral colour distribution for 134 galaxies in the measured field for which the  $B-V$  colours have been measured. No field correction has been applied. In the figure the number of galaxies is plotted against  $B-V$  in  $0^m.2$  bins. Some features in this distribution may be pointed out. Firstly the integral colours range in a broad interval from zero up to about  $1^m.8$ . Secondly, there is a broad maximum around the value  $0^m.9$ . Finally, there is a well defined cut-off at the red end of the histogram at  $B-V=1.2$ . In Fig. 5b the distribution of nuclear colours measured in a radius of 3 arcsec is given. There are some nuclei with  $B-V$  near zero. Contrary to Fig. 5a the red end of the histogram decreases gradually.

To investigate the colour segregation effect, galaxies of Fig. 4a have been divided in two groups: those with  $B-V < 0.7$  and those

with  $B - V > 0.7$ . The ratio  $N_{B-V < 0.7} / N_{B-V > 0.7}$  in different rings will show the colour segregation effect. The results are given in Table 3.

Table 3

COLOUR SEGREGATION EFFECT IN THE CLUSTER  
A1185

The Ring Radius	$N_{B-V < 0.7}$	$N_{B-V > 0.7}$	$\frac{N_{B-V < 0.7}}{N_{B-V > 0.7}}$
0-0.12	7	36	0.19
0.12-0.24	20	35	0.67
0.24-0.33	15	22	0.68

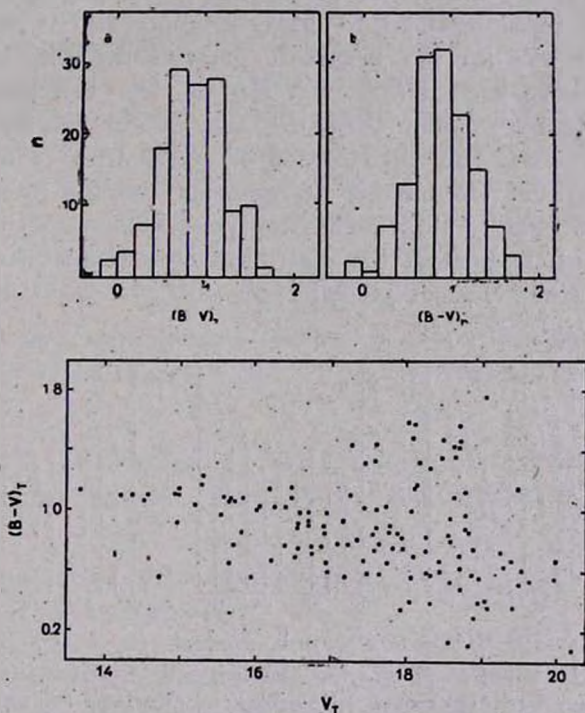


Fig. 5. Colour distribution of galaxies; a) for integral colours; b) for nuclear colours; c) Magnitude-colour relation.

From these data one can see that there is a lack of bluer galaxies in the central region of the cluster in comparison to the outer parts. It means that the central part of the cluster consists of mainly elliptical and lenticular galaxies. The application of the field correction will not change this result significantly.

d) *Magnitude-Colour Relation.* This relation is shown in Fig. 5c. We see that the brightest galaxies in the cluster in the mean are redder than the fainters. Some of the galaxies fainter than  $17^m.5$  have large  $B-V$ . Apparently most of these objects are background galaxies. If one excludes these objects, the change of  $B-V$  in the observed range of magnitudes amounts to  $0^m.5$ . Thus less luminous galaxies in the cluster are bluer.

e) *The distribution of ellipticities and position angles.* To determine the ellipticity of a galaxy two criteria have been applied. Firstly, the range of surface magnitudes in the galaxy has been divided into several intervals of  $1^m$  width each, the faintest surface brightness being  $24^m.5$ . Secondly, the number of pixels in a given magnitude interval has been taken to be at least 20 to have a good fit of isophotes to an ellipse. In this way for the brightest galaxies the ellipticities of several isophotes have been determined. For the few brightest galaxies the outer isophotes are rounder than the inner. For fainter galaxies both cases equally exist. The distribution of ellipticities of outer isophotes is given in Fig. 6a. The number of galaxies per 0.1 interval in ellipticity is plotted against ellipticity. The peak at  $\epsilon = 0.35$  is not statistically significant. In general the distribution does not differ significantly from that in other clusters [4, 25].

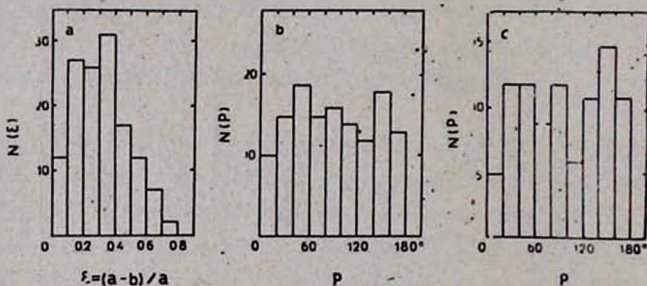


Fig. 6. a) Distribution of apparent ellipticities; b) distribution of position angles for all galaxies with measured ellipticities; c) the same for galaxies with ellipticities larger than 0.2.

The position angles of large axes of galaxies have been determined by means of the same fitted ellipses as the ellipticities. Fig. 6b shows the distribution of position angles of the largest axes of 132 galaxies. In this histogram all galaxies with measured position angles are used independently from the magnitude of ellipticity. The position angle of the brightest galaxy NGC 3550 is  $65^\circ$ . As observed the distribution is

fairly uniform. However there appears some minima and maxima when galaxies with  $\epsilon > 0.2$  are considered (Fig. 6c) Since the number of galaxies per interval is not large enough it is difficult to claim the non-uniformity of this distribution.

5. *Conclusions.* According to Table 1 in a circle of radius 0.7 Mpc studied in this work there exist 30 galaxies in a magnitude interval ( $m_3, m_3 + 2$ ) where  $m_3$  is the magnitude of third brightest galaxy in the cluster. For clusters of richness class 1 Abell [8] gives from 50 to 79 galaxies in the same magnitude interval whereas in a circle of 2 Mpc in radius. Taking into account the difference in the surfaces and the rate of decreasing of galaxy density with radius (Fig. 3) we can only confirm that the cluster A1185 belongs to the richness class 1. The brightest cluster galaxy NGC 3550 is a supergiant with  $M_V = -22.1$ . According to Zwicky [26] it is a galaxy with a double nucleus. On our plates besides the two bright condensations a fainter isolated condensation is seen south-west of the center. All three condensations are aligned from north-east to south-west. The distance between two extreme condensations is 21.4 or  $\sim 14$  kpc. We can say that NGC 3550 has a triple nucleus two of which are comparable in luminosity while the third one being less luminous.

The main results of this paper may be summarized as followings.

1. There is a well defined change of slope in logarithmic cumulative luminosity functions in  $B$  and  $V$ . The intersection point in  $V$  is at  $M_V^* = -20.0$ .

2. There is a remarkable radial segregation both in luminosity and colour in the cluster, the brighter and redder galaxies are more concentrated.

3. No convincing evidence has been found for preferential alignments of major axes of galaxies.

It is a pleasure to extend our gratitude to Prof. V. A. Ambartsumian for the useful discussion, A. S. Amirkhanian for help in observations, V. A. Yakovleva and S. V. Sudakov for observations of photoelectric magnitudes of some faint stars in IC 4665.

One of the authors (A. T. K.) is grateful to the staff of Rome and Naples Observatories for hospitality and to the National Research Council of Italy for financial support.

Byurakan Astrophysical  
Observatory  
Osservatorio Astronomico  
di Roma

## ДВУХЦВЕТНАЯ ФОТОМЕТРИЯ СКОПЛЕНИЙ ГАЛАКТИК. I. A1185

А. Т. КАЛЛОГЛЯН, А. Г. ЕГИКЯН, Д. НАННИ, Д. ТРЕВЕЗЕ, А. ВИНЯТО

Приводятся результаты двухцветной фотометрии галактик скопления А 1185 в системе  $B$ ,  $V$ . Используются снимки 2.6-м телескопа Бюраканской обсерватории. Измерения производились на микроденситометре Неапольской обсерватории. Определены прямоугольные координаты, интегральные звездные величины и цвета, эллиптичности и позиционные углы больших осей галактик. Построена функция светимости в  $B$  и  $V$ . В кумулятивной функции светимости имеется излом в точках с  $M_B = -19.0$  и  $M_V = -20.0$  в  $B$  и  $V$  соответственно. Нет определенного свидетельства о наличии преимущественной ориентации у больших осей галактик скопления. Более яркие и более красные галактики сильнее концентрируются к центру скопления.

### REFERENCES

1. A. Jr. Oemler, Ap. J., 194, 1, 1974.
2. A. M. Dressler, Ap. J., 223, 765, 1978.
3. J. G. Godwin, J. V. Peach, M. N. RAS., 181, 323, 1977.
4. D. Carter, M. N. RAS., 190, 307, 1980.
5. D. Carter, J. G. Godwin, M. N. RAS., 187, 711, 1979.
6. A. A. Hoffman, Ph. Crans, Ap. J., 215, 379, 1977.
7. R. G. Kron, Ap. J., Suppl. ser., 43, 305, 1980.
8. G. O. Abell, Ap. J. Suppl. ser., 3, 211, 1958.
9. A. A. Lehr, S. van den Bergh, Ap. J. Suppl. ser., 34, 381, 1977.
10. T. W. Noonan, Ap. J., Suppl. ser., 45, 613, 1981.
11. F. N. Owen, A. J., 79, 427, 1974.
12. H. M. Johnson, Ap. J. Suppl. ser., 47, 235, 1981.
13. J. D. McKee, R. F. Mushotzky, E. A. Boldt, S. S. Holt, F. E. Marshall, S. H. Pravdo, P. J. Serlemittos, Ap. J., 242, 843, 1980.
14. И. Д. Караченцев, А. Л. Щербановский, Астрон. ж., 55, 449, 1978.
15. G. Pittella, A. Vignato, Mem. S. A. It., 50, 537, 1979.
16. B. A. Peterson, A. J., 75, 695, 1970.
17. D. Carter, N. Metcalfe, M. N. RAS., 191, 325, 1980.
18. J. J. Lirre, W. D. Benton, D. A. Elliot, Proc. SPIE, 172, 394, 1979.
19. E. Valders, The Resolution Classifier, 1983 (in press).
20. B. A. Peterson, R. S. Ellis, E. J. Kibblewhite, M. T. Bridgeland, T. Hooley, D. Horns, Ap. J., 233, L109, 1979.
21. D. Nanni, G. Pittella, D. Treves, A. Vignato, Proc. SPIE, 264, 48, 1980.
22. И. Д. Караченцев, А. И. Копылов, Письма АЖ, 3, 246, 1977.
23. P. Schechter, Ap. J., 203, 297, 1976.
24. G. O. Abell, Ap. J., 213, 327, 1979.
25. H. T. MacGillivray, R. J. Dodd, M. N. RAS., 186, 743, 1979.
26. F. Zwicky, E. Herzog, Catalogue of Galaxies and of Clusters of Galaxies, II. Switzerland, 1963.